Journal of Power Sources 256 (2014) 32–36

Contents lists available at ScienceDirect

Journal of Power Sources

journal homepage: www.elsevier.com/locate/jpowsour

Short communication

From Si wafers to cheap and efficient Si electrodes for Li-ion batteries

Magali Gauthier [a,b,c], David Reyter [a], Driss Mazouzi [b,c], Philippe Moreau [b,c], Dominique Guyomard [b,c], Bernard Lestriez [b,c], Lionel Roué [a,*]

[a] INRS-Énergie, Matériaux, Télécommunications, 1650 boulevard Lionel Boulet, Varennes, QC J3X 1S2, Canada
[b] Institut des Matériaux Jean Rouxel (IMN), Université de Nantes, CNRS, 2 rue de la Houssinière, BP 32229, 44322 Nantes Cedex 03, France
[c] Réseau sur le Stockage Electrochimique de l'Energie (RS2E), FR CNRS 3459, France

HIGHLIGHTS

- This work provides a cheap and green way to produce Si anodes for Li-ion batteries.
- Ball-milled Si wafer is used as active material.
- 900 cycles at 1200 mAh g^{-1} of Si are achieved.

GRAPHICAL ABSTRACT

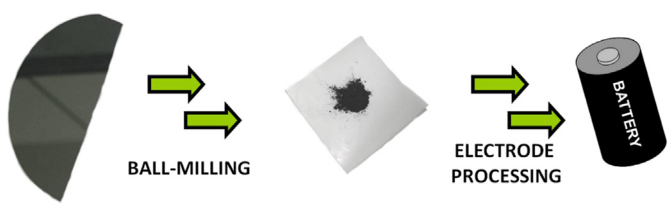

ARTICLE INFO

Article history:
Received 26 November 2013
Received in revised form
7 January 2014
Accepted 8 January 2014
Available online 15 January 2014

Keywords:
Li-ion batteries
Silicon electrodes
Si wafer
Ball milling

ABSTRACT

High-energy ball milling is used to recycle Si wafers to produce Si powders for negative electrodes of Li-ion batteries. The resulting Si powder consists in micrometric Si agglomerates made of cold-welded submicrometric nanocrystalline Si particles. Silicon-based composite electrodes prepared with ball-milled Si wafer can achieve more than 900 cycles with a capacity of 1200 mAh g^{-1} of Si (880 mAh g^{-1} of electrode) and a coulombic efficiency higher than 99%. This excellent electrochemical performance lies in the use of nanostructured Si produced by ball milling, the electrode formulation in a pH 3 buffer solution with CMC as binder and the use of FEC/VC additives in the electrolyte. This work opens the way to an economically attractive recycling of Si wastes.

1. Introduction

For a few years, great attention has been paid to silicon as a negative electrode material for Li-ion batteries, due to its very high gravimetric and volumetric capacities (3572 mAh g^{-1} and 8322 mAh cm^{-3}) in comparison to graphite (372 mAh g^{-1} and 818 mAh cm^{-3}) [1]. However, unoptimized Si electrodes suffer from poor cyclability due to the large volumetric expansion of Si particles upon cycling, resulting in their pulverization and electrical disconnection [2], and to the formation of an unstable solid electrolyte interphase (SEI) leading to low coulombic efficiencies [3–5]. Several approaches have been proposed in the literature to solve these issues, such as the limitation of the delivered capacity [1,6], the use of appropriate binders [7,8] and electrolytes additives [5,9,10], and the use of Si nanoparticles or nanostructures [11]. This last one is very popular in the academic community and is thought to be essential to obtain a good cyclability of Si electrodes. Nevertheless, we have recently demonstrated the ability to produce low-cost and efficient silicon-based electrodes by using micrometric Si powders produced by high-energy ball milling (HEBM) of a nearly millimetric silicon powder [12]. By combining the nanostructuration created by HEBM, the processing of the electrode at pH 3 with CMC (carboxymethylcellulose) binder and the use of fluoroethylene and vinylene carbonates (FEC/VC) electrolyte additives, remarkable performance was achieved. Close to 900 cycles were obtained with a capacity limited to 1200 mAh g^{-1} of silicon for an active mass loading of about 1 mg cm^{-2} [12].

* Corresponding author. Tel.: +1 514 228 6985; fax: +1 450 929 8102.
E-mail address: roue@emt.inrs.ca (L. Roué).

0378-7753/$ – see front matter
http://dx.doi.org/10.1016/j.jpowsour.2014.01.036

Herein, we show that similar electrochemical performance can be reached using Si wafer as starting material, providing a cheap and green way to produce Si-based electrodes from Si wafer scraps coming from the semiconductor and photovoltaic industries. A large amount of Si wafer scraps is produced by the semiconductor and photovoltaic industries. For instance, with a 3.3% scrap rate (based on IBM semiconductor manufacturing data) applied to all started wafers worldwide annually, at least 3 millions are scrapped per year [13]. As demonstrated in the present study, these cheap scraps could be recycled to produce high performance Si-based anodes, reducing the precursor cost and saving the energy needed for a new silicon material source (which translates into an overall reduction of the carbon footprint). In addition, we want to stress that ball milling is a very cheap process. Indeed, its cost has been estimated at ~2 € per kg of Si for a daily capacity of 100 kg [12], which is by far cheaper that the common ways of production (*e.g.* chemical vapor deposition) of nanometric Si particles for Li batteries.

2. Experimental

2.1. Synthesis

A commercial silicon wafer (Fig. 1) (p-type, 10–20 Ω cm^{-1}) was used as starting material. It was first crushed in small pieces with a hammer and then introduced along with 3 stainless-steel balls (one of 14.3 mm and two of 11.1 mm diameter) into a stainless-steel vial (55 mL). The ball-to-powder mass ratio was 5:1. HEBM was carried out under argon at room temperature for 20 h using a SPEX 8000 mixer. The milling yield (defined as the ratio of the powder masses after and before milling) was higher than 90%, reflecting limited cold welding between the powder and the milling tools. Only 0.23 wt.% of iron was detected in the milled wafer powders by neutron activation analysis, indicating the absence of significant iron contamination from the erosion of the container and balls during milling. The oxygen content (measured with a LECO oxygen analyzer) in the milled Si was 1.05 wt.%.

2.2. Electrochemical measurements

Composite electrodes were fabricated with milled Si wafer powder (Fig. 1) as active material, Super P carbon black (noted CB, TIMCAL) as conductive agent and CMC (DS = 0.7, Mw = 90,000, Aldrich) as binder. A mixture of 200 mg of active material + CB + CMC in a weight proportion of 80:12:8 was introduced along with 0.5 mL of a buffer solution at pH 3 (citric acid + KOH) and three silicon nitride balls into a silicon nitride vial. Mixing was performed at 500 rpm for 1 h using a Fritsch Pulverisette 7 mixer. The slurry was then tape cast with a doctor blade onto a 25 μm thick copper foil, dried at room temperature for 12 h and then at 100 °C in vacuum for 2 h. No calendar pressure was used. Citric acid and KOH from the buffer solution did not evaporate during the drying process and thus contribute to the mass of electrodes, leading to a Si/CB/CMC/(citric acid + KOH) wt.% composition of 73.1/11.0/7.3/8.6. The Si mass loading was about 0.9 mg cm^{-2} and the electrode density was about 0.7 g cm^{-3}. Two-electrode Swagelok®-type cells were used to perform cycling tests in a galvanostatic mode at 20 °C between 1 and 0.005 V versus Li^+/Li^0 using a VMP automatic cycling/data recording system (Biologic Co.). Cells were assembled in an argon-filled glove box and comprise: (i) a 0.785 cm^2 disc of the composite working electrode; (ii) a Whatman GF/D borosilicate glass-fiber separator soaked with a 1 M $LiPF_6$ electrolyte dissolved in 1:1 ethylene carbonate (EC)/diethyl carbonate (DEC) with 10 wt.% FEC and 2 wt.% VC; and (iii) a 1 cm^2 Li metal disc as the counter and reference electrode. Otherwise mentioned, electrodes were cycled with a limited capacity of 1200 mAh g^{-1} of Si (880 mAh g^{-1} of electrode) at a rate of 1 lithium in 1 h (C) both in discharge (lithiation) and charge (delithiation), corresponding to a current density of 960 mA g^{-1} of silicon.

Fig. 1. View of the Si wafer before and after high-energy ball-milling.

2.3. Characterization

Morphological and structural characterizations were performed by scanning electron microscopy (SEM) using a JEOL JSM-6300F microscope, and by transmission electron microscopy (TEM) using a Hitachi HNAR9000 microscope operated at 300 kV. The laser scattering method was used to determine the particle size distribution in aqueous media using a Mastersizer 2000 Malvern analyzer. X-ray diffraction (XRD) measurements were performed with a Bruker D8 diffractometer using the Cu Kα radiation (λ = 154.0598 pm).

3. Results and discussion

HEBM of the Si wafers has been conducted under argon atmosphere for 20 h (Fig. 1). SEM image and particle size distribution of the Si powder obtained after the milling process are presented in Fig. 2a and b, respectively. Three populations of particle size around 100 nm, 1 μm and 30 μm appear in Fig. 2b. As observed with our milled commercial powders [12], the powder appears micrometric (Fig. 2a) but is constituted of agglomerates of particles of the order of a few hundred nanometers. Due to the effect of the repeated fracturing and welding that took place during the milling process, many defects and dislocations are observed on the milled powder, as highlighted in the high resolution TEM image in Fig. 3a. Various crystalline orientations can be spotted (see Fig. 3a, lines) and as a result, a lot of crystalline domains (circles) and grain boundaries exist in the powder. From our TEM images, the crystallite size of these domains can be estimated at around 10 nm, which is consistent with our previous study on milled commercial powders [12] and with the mean value of 10 nm calculated from all the reflections of the XRD pattern (Fig. 3b) using the Sherrer–Wilson formula [14]. XRD patterns underline also the fact that, as expected, the Si crystal structure of Si wafers is completely changed after the milling process. Before milling, the XRD pattern displays only the (100) peak at around 69°, which corresponds to the initial crystalline orientation of the Si wafer. On the other hand, after the milling process, all the characteristic peaks of Si are detected and appear much broader. This is related to the decrease of the crystallite size, and to a lesser extent, to a rise of the lattice strain with the milling process. Note that no impurities are detected before and after the milling process by XRD.

We assumed that, thanks to the nanostructuration created by the milling process, a more gradual volume variation of the Si milled particles could occur during lithiation/delithiation cycling,

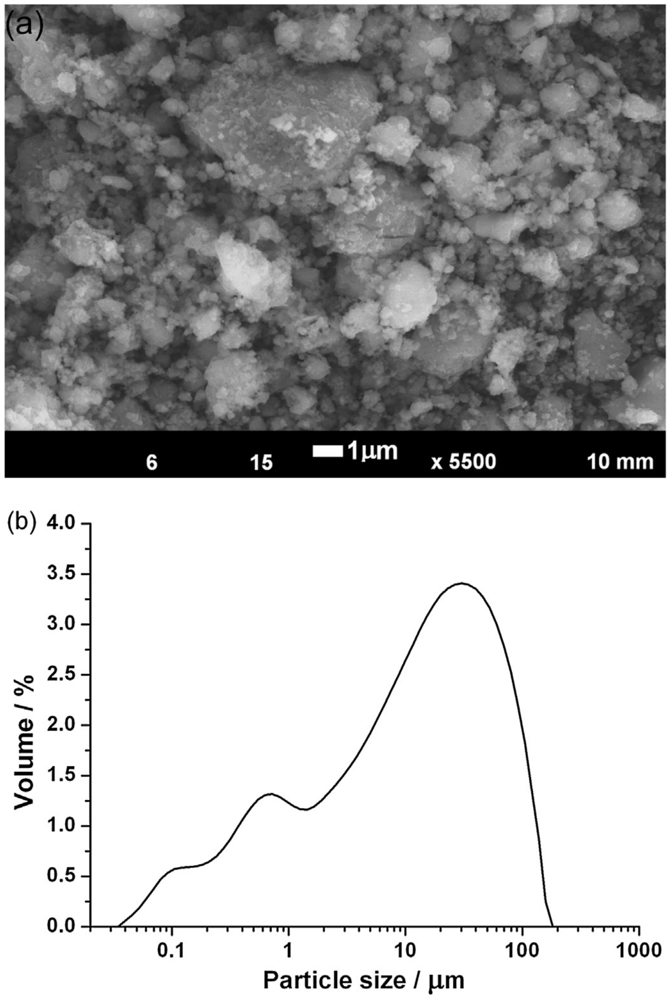

Fig. 2. (a) SEM micrograph and (b) particle size distribution of the ball-milled Si wafer powder.

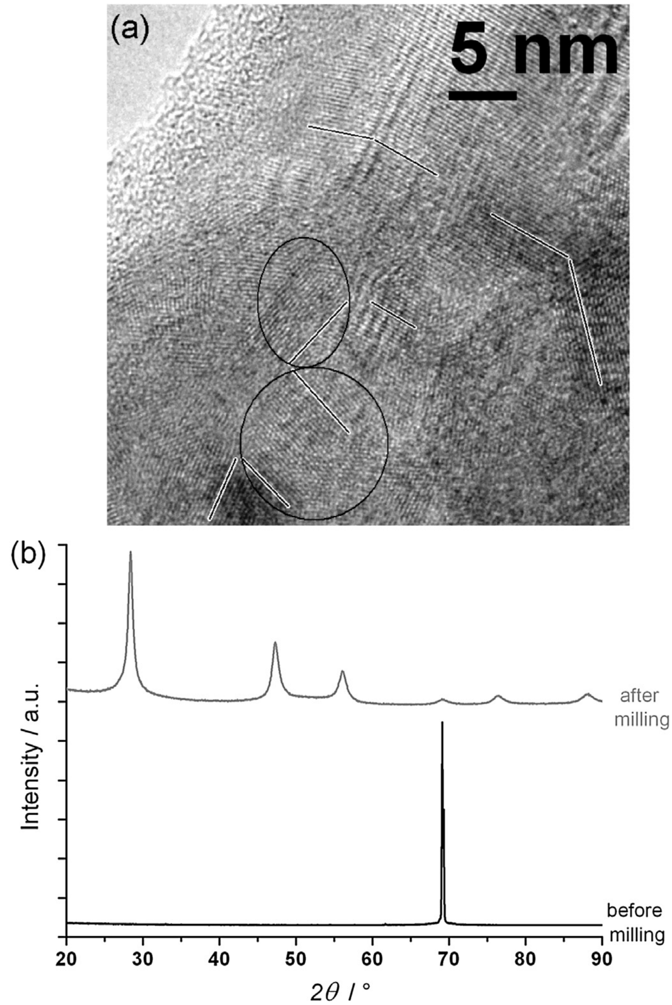

Fig. 3. (a) TEM image of the ball-milled Si wafer powder (nanocrystalline domains are visualized by circles and crystalline orientations are marked with white edged black lines) and (b) XRD patterns of the Si wafer before and after milling.

which may limit the cracking and disconnection of the Si particles as well as the rupture of the SEI surface layer [12]. The large particle size distribution of the milled Si material and resulting appropriate particle packing in the composite electrode may also favor an efficient electronic network for insuring the electrode stability upon cycling.

Electrochemical cycling tests were performed on this nanostructured micrometric powder in the range 5 mV–1 V with metallic lithium at the counter electrode. In order to optimize the cycling performance, electrodes were prepared with conductive carbon and CMC in a pH 3 buffer solution, this latter promoting the covalent bonding of CMC with Si [15]. In addition, FEC and VC were added to the electrolyte in order to stabilize the SEI upon cycling [5]. Finally, the discharge capacity was limited to 1200 mAh g^{-1} of Si to minimize decrepitation of Si particles. Fig. 4a presents the evolution of the electrode discharge capacity with cycling at a current density of 960 mA g^{-1}. The electrode exhibits an impressive stability for 900 cycles of charge/discharge with a constant discharge capacity of 1200 mAh g^{-1} of Si. Voltage profiles corresponding to cycles 1, 2, 10, 500 and 900 of Fig. 4a are displayed in Fig. 4b. A quite low coulombic efficiency of 59.8% is obtained for the first cycle, corresponding to an irreversible capacity of 480 mAh g^{-1} of Si (Fig. 4b). This large first cycle irreversible capacity is related to the SEI formation and to the reaction of the native oxide layer on Si particles with lithium. Apart from the first ten cycles where the irreversible losses are higher (Fig. 4b), the coulombic efficiency is comprised between 99.2 and 99.9% during all the cycling. As highlighted in our previous study [12], we consider that such high performance (900 cycles at 1200 mAh g^{-1} of Si) results from the nanostructuration generated by the milling process and in the joint contribution of CMC binder at pH 3 and FEC/VC electrolyte additives. Cycling experiments were also performed with no capacity limitation (not shown), leading to a capacity of 2250 mAh g^{-1} of Si at the 250th cycle. These performance data are comparable to those obtained with milled commercial (1–5 µm or 20 mesh) Si powders [12]. This confirms that the electrochemical behavior of milled Si material is independent of the particle size/shape of the starting material. It must also be noted that lower performance was obtained with commercial nanometric (50 nm) Si powder cycled in similar conditions, displaying a capacity retention of 1200 mAh g^{-1} for 650 cycles [12] compared to 900 cycles for milled Si powder or wafer.

Differential capacity profiles measured upon cycling of Fig. 4a confirm the exceptional stability of the milled Si wafer electrode (Fig. 4c). Focusing on the oxidation part of the curves, solely the peak labeled *A* is clearly present until the fall of the capacity, whereas the peak *B* is almost inexistent. This is remarkable considering that the usual path for the capacity fade during cycling is an increase of peak *B*, corresponding to lithium-richer $SiLi_x$ alloys

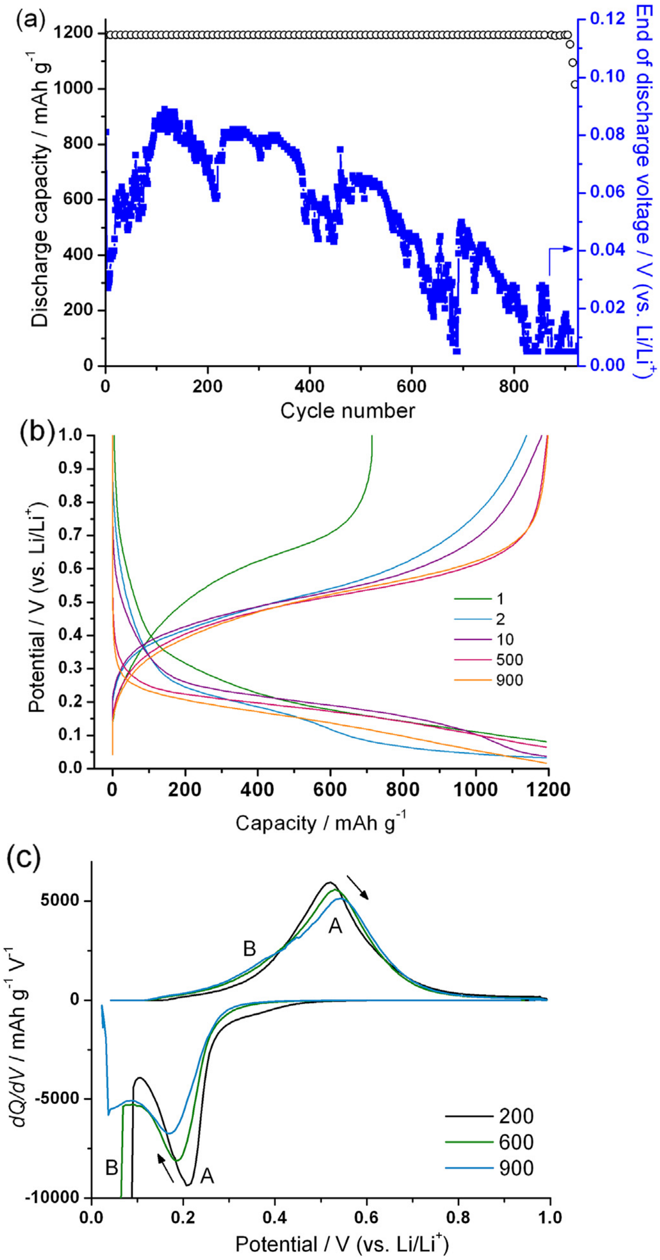

Fig. 4. (a) Evolution with cycling of discharge capacities and end-of-discharge voltage of milled Si wafers based electrodes with capacity limitation to 1200 mAh g^{-1} of Si in FEC/VC containing electrolyte. (b) Voltage profiles corresponding to cycles 1, 2, 10, 500 and 900 of figure (a). (c) Differential capacity profiles corresponding to cycles 200, 600 and 900 of figure (a). The electrode Si loading is approximately 0.9 mg cm^{-2}. The rate is 1Li/Si in 1 h, corresponding to a current density of 960 mAh g^{-1} of Si. Capacities are given per gram of Si.

than for peak *A*, concomitant with the decrease of peak *A* intensity [4]. This was explained by the gradual disconnection of Si particles during cycling (which no longer take part in the capacity), leading to a deeper lithiation of the remaining active particles in order to deliver the desired capacity. In the case of the milled Si wafer based electrode, step *B* is almost inexistent over 900 cycles, which means that alloying/dealloying processes are spread evenly between all particles in the electrode. Consequently, pulverization and disconnection of Si particles seem to be very limited in the milled Si wafer electrode. The fall of the electrode capacity cannot thus be explained by the pulverization of the electrode upon cycling but rather by a progressive increase of the electrode polarization [5]. This agrees with the evolution of the end-of-discharge potential with cycling of the Si wafer electrode presented in Fig. 4a. As previously observed [4,15], the end-of-discharge potential decreases during cycling, finally dropping to the cut-off voltage (0.005 V). The capacity drop occurring beyond 900 cycles coincides with the point where the potential reaches the cut-off voltage. The rise of the electrode polarization is thus most likely responsible for the end of life of the electrode. This electrode polarization increase is further confirmed by the shifts of the peak potential in the incremental curves (Fig. 4c), especially in the cathodic part where Li^+ mass transport constraints in the pores of the composite electrode occur. Mazouzi et al. [5] have already demonstrated that the increase of the irreversible capacity loss with cycling is related to the growth of the electrode's mass and thickness due the continuous accumulation of insoluble solvent degradation products as recently confirmed by nuclear magnetic resonance (NMR) analyses [16]. Actually, it is reasonable to assume that this phenomenon accounts for the increase of the electrode polarization with cycling coming from gradual obstruction of the composite electrode pores, thus hindering the diffusion of Li ions into the electrode [4,5]. As a consequence, we believe that this material could have unlimited cycle life if an ideal surface treatment or electrolyte composition inducing the formation of a stable SEI could be discovered.

High rate performance of the milled Si wafer based electrodes was also investigated, with a discharge capacity limited to 1200 mAh g^{-1} (Fig. 5). Discharge/charge rates of C/10 to 10C were applied, corresponding to current densities of 0.096–9.6 A g^{-1}, respectively. The milled Si wafer electrode exhibits a constant discharge capacity of 1200 mAh g^{-1} from C/10 to C rates. The discharge capacity retention is around 75% at a rate of 2C (1.92 A g^{-1}) and 30% at a rate of 5C (4.8 A g^{-1}). For comparison, a capacity retention of about 75% (~900 mAh g^{-1}) at a rate of 4.8 A g^{-1} was obtained with Si nanotube based electrode, with however a much lower Si loading (0.02–0.1 mg cm^{-2}) than in the present study (~1 mg cm^{-2}) [17].

4. Conclusion

We showed that Si wafer scraps can be recycled to produce Si-based electrodes for Li-ion batteries using an easy and cheap process. High-energy ball milling of Si wafers produces micrometric

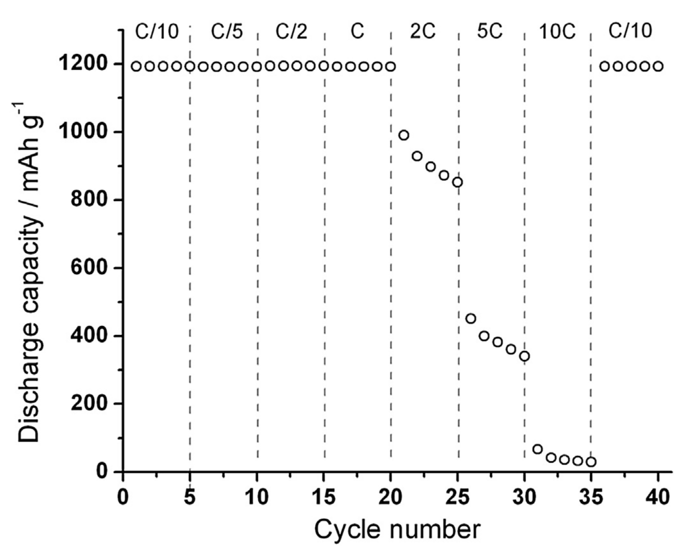

Fig. 5. Rate performance of milled Si wafers based electrodes for a discharge capacity limited to 1200 mAh g^{-1} in FEC/VC containing electrolyte. The electrode Si loading is 0.9 mg cm^{-2}. A rate of 1C corresponds to 1Li/Si in 1 h (*i.e.*, 960 mA g^{-1}) in discharge and charge.

but nanostructured Si powders that present tremendous performance when used in optimized composite electrodes and electrolyte solutions. These kinds of powders present the same benefits of nanometric Si in terms of performance but not the drawbacks: toxicity, handling difficulties and above all, cost. We think this painless method of producing Si powders is a way to recycle Si wafer scraps from photovoltaic or electronic industries and to reduce cost of Si electrodes for Li-ion batteries. The next step of this work will be to reduce the irreversibility generated during cycling and to prepare electrodes with high Si loadings in order to obtain practical electrodes for Li-ion batteries.

Acknowledgments

Financial funding from the Agence Nationale de la Recherche (ANR) of France (BASILIC project) and the Natural Science and Engineering Research Council (NSERC) of Canada is acknowledged.

References

[1] M.N. Obrovac, L.J. Krause, J. Electrochem. Soc. 154 (2007) A103–A108.
[2] J.H. Ryu, J.W. Kim, Y.E. Sung, S.M. Oh, Electrochem. Solid-State Lett. 7 (2004) A306–A309.
[3] M. Winter, Z. Phys. Chem. 223 (2009) 1395.
[4] Y. Oumellal, N. Delpuech, D. Mazouzi, N. Dupre, J. Gaubicher, P. Moreau, P. Soudan, B. Lestriez, D. Guyomard, J. Mater. Chem. 21 (2011) 6201–6208.
[5] D. Mazouzi, N. Delpuech, Y. Oumellal, M. Gauthier, M. Cerbelaud, J. Gaubicher, N. Dupré, P. Moreau, D. Guyomard, L. Roué, B. Lestriez, J. Power Sources 220 (2012) 180–184.
[6] U. Kasavajjula, C. Wang, A.J. Appleby, J. Power Sources 163 (2007) 1003–1039.
[7] B. Lestriez, S. Bahri, I. Sandu, L. Roué, D. Guyomard, Electrochem. Commun. 9 (2007) 2801–2806.
[8] I. Kovalenko, B. Zdyrko, A. Magasinski, B. Hertzberg, Z. Milicev, R. Burtovyy, I. Luzinov, G. Yushin, Science 334 (2011) 75–79.
[9] N.-S. Choi, K.H. Yew, K.Y. Lee, M. Sung, H. Kim, S.-S. Kim, J. Power Sources 161 (2006) 1254–1259.
[10] R. Elazari, G. Salitra, G. Gershinsky, A. Garsuch, A. Panchenko, D. Aurbach, J. Electrochem. Soc. 159 (2012) A1440–A1445.
[11] J.R. Szczech, S. Jin, Energy Environ. Sci. 4 (2011) 56–72.
[12] M. Gauthier, D. Mazouzi, D. Reyter, B. Lestriez, P. Moreau, D. Guyomard, L. Roué, Energy Environ. Sci. 6 (2013) 2145–2155.
[13] http://www-03.ibm.com/press/us/en/pressrelease/22504.wss, (accessed 26.11.13).
[14] H.P. Klug, L.E. Alexander, X-ray Diffraction Procedures for Polycrystalline and Amorphous Materials, John Wiley & Sons, New York, 1974.
[15] D. Mazouzi, B. Lestriez, L. Roué, D. Guyomard, Electrochem. Solid State Lett. 12 (2009) A215–A218.
[16] N. Delpuech, N. Dupré, D. Mazouzi, J. Gaubicher, P. Moreau, J.S. Bridel, D. Guyomard, B. Lestriez, Electrochem. Commun. 33 (2013) 72–75.
[17] H. Wu, G. Chan, J.W. Choi, I. Ruy, Y. Yao, M.T. McDowell, S.W. Lee, A. Jackson, Y. Yan, L. Hu, Y. Cui, Nat. Nanotechnol. 7 (2012) 310–315.